ISSN 1063-7826, Semiconductors, 2006, Vol. 40, No. 9, pp. 1036–1042. © Pleiades Publishing, Inc., 2006.
Original Russian Text © V.D. Kalganov, N.V. Mileshkina, E.V. Ostroumova, 2006, published in Fizika i Tekhnika Poluprovodnikov, 2006, Vol. 40, No. 9, pp. 1062–1068.

SEMICONDUCTOR STRUCTURES, INTERFACES, AND SURFACES

Tunneling Emission of Electrons from Semiconductors' Valence Bands in High Electric Fields

V. D. Kalganov[a], N. V. Mileshkina[a], and E. V. Ostroumova[b]^

[a]*Fock Research Institute of Physics at the St. Petersburg State University (Petrodvorets Branch), Universitetskiĭ pr. 2, Petrodvorets, 198904 Russia*

[b]*Ioffe Physicotechnical Institute, Russian Academy of Sciences, Politekhnisheskaya ul. 26, St. Petersburg, 194021 Russia*

^e-mail: elena.ostroumova@mail.ioffe.ru

Submitted November 24, 2005; accepted for publication December 8, 2005

Abstract—Tunneling emission currents of electrons from semiconductors to vacuum (needle-shaped GaAs photodetectors) and to a metal (silicon metal–insulator–semiconductor diodes with a tunneling-transparent insulator layer) are studied in high and ultrahigh electric fields. It is shown that, in semiconductors with the *n*-type conductivity, the major contribution to the emission current is made by the tunneling emission of electrons from the valence band of the semiconductor, rather than from the conduction band.

PACS numbers: 79.70.+q, 79.60.Jv

DOI: 10.1134/S1063782606090089

1. INTRODUCTION

Studies of the charge transport in semiconductors in high electric fields, $(2–5) \times 10^7$ V/cm, and, in particular, tunneling emission of electrons from semiconductors have recently attracted not only theoretical but also practical interest in relation to the development of high-speed semiconductor devices for microelectronics, nanoelectronics, and optoelectronics. We have previously studied both (i) the tunneling emission of electrons from semiconductors into vacuum in the field and photofield semiconductor emitters (Ge, InSb, and GaAs) and (ii) the electron injection from metal into semiconductor in an Auger transistor (the Al–SiO_2–*n*-Si structures with the tunneling-transparent insulator layer); these studies made it possible to identify the specific features of the tunneling-emission physical mechanism in these devices and reveal the common trends [1, 2]. It was shown that, in both cases, the tunneling current is governed by the density of minority charge carriers in self-aligned quantum wells (QWs) that emerge at the semiconductor surface in high electric fields. The tunneling current is identified with the electron current from the valence band of the *p*-type semiconductor into vacuum for a field-assisted emitter that operates in the mode of a photofield detector and with the tunneling injection current of electrons from the metal into the conduction band of the *n*-type semiconductor in the case of the metal–insulator–semiconductor (MIS) structure in the Auger transistor.

However, according to the available publications, a quantity-produced operating Auger transistor has not been fabricated yet; a complete theoretical model of this transistor is also lacking. A quantum-mechanical model of the tunneling electron current in *p*-type semiconductors in the high and ultrahigh electric fields has not been developed so far despite the fact there are numerous experimental data published. In addition, the mechanism of sharp increase in the quantum efficiency to the values of >100% in the field-assisted photodetectors in high electric fields under illumination has not been identified with confidence.

Studies of recombination radiation of silicon MIS diodes with the tunneling-transparent insulator (oxide) layer and various metals (at forward-bias voltage applied to the structure) showed that, in the case of high current densities, the efficiency of the wide-gap emitter, which is exactly represented by the metal–oxide–semiconductor (MOS) heterojunction, is close to unity and does not decrease as the current density increases up to 150 A/cm^2. Compared to the silicon p^+–*n* diffusion homojunctions, the current range where the injection factor is close to unity is wider by an order of magnitude owing to the unidirectional tunneling injection of minority charge carriers (electrons) from the semiconductor's valence band into metal in tunneling MIS diodes based on silicon with *n*-type conductivity [3].

These results brought into existence the Auger transistor based on the Al–SiO_2–*n*-Si tunneling structures with the quantum-dimensional *p*-type base induced by the electric field in the oxide and represented by a self-consistent QW for holes [4, 5]. The induced *p*-type layer has the thickness of ~10^{-7} cm. The energy of injected electrons consists of two components; one component is related to the voltage drop across the oxide and the other, to the voltage drop across the base layer. The second component can attain values that are comparable with the silicon band gap. The principle of

operation of an Auger transistor is based on an increase in the current gain α to a value in excess of unity ($\alpha > 1$) as a result of the generation of electron–hole (e–h) pairs in the course of impact ionization by hot electrons injected from the metal. The e–h pairs are generated in the semiconductor's surface region at a distance of ~100 Å from the oxide–silicon interface [5, 6]. The presence of the tunneling-transparent oxide layer on the semiconductor surface makes it possible to attain electric-field strength as high as $(3–5) \times 10^7$ V/cm in the structure's surface region at a bias voltage applied to the oxide no higher than 2 V and to obtain the unidirectional injection of hot electrons from the metal into the semiconductor. It is the development of the Auger transistor that makes it possible to study the tunneling emission of hot electrons in the MIS structures in high electric fields.

It is worth noting that the concept of dimensional quantum effects in the aforementioned self-aligned QWs at the surface of semiconductors is widely used in solid-state electronics [7]. However, realization of these effects in the case of the field-assisted tunneling emission for electrons moving perpendicularly to the surface is not evident in the typically studied situations, where the probability of penetration through the barrier is finite. This issue remains to be solved and verified experimentally.

From the practical standpoint, the study of the MIS tunneling structures has made it possible to gain insight into the conditions for the hot-electron emission from the metal to the semiconductor and into additional heating of these electrons in the self-aligned QW at the surface; in turn, this study was conducive to the development of the Auger transistor based on the Al–SiO_2–n-Si heterojunction, which has at present the highest speed of response among the bipolar semiconductor transistors [4–6].

At the same time, the practical result of studying the tunneling emission from a semiconductor to vacuum at various currents and at different levels of illumination consisted in the development of field-assisted photocathodes whose quantum efficiency can appreciably exceed 100%; these photocathodes can operate successfully in the infrared spectral region [8, 9].

The unidirectional injection of electrons in an Auger transistor is a consequence of the fact that, due to a large effective mass of holes in the valence band of silicon oxide, the hole current is negligible compared to the current of tunneling injection of electrons from the metal. In contrast, as is known, only electron current exists in vacuum. However, experiments show that the efficiency of emission of electrons from a p-type semiconductor is as high as that from an n-type semiconductor. The effect of an increase in the quantum efficiency in illuminated tips for the p-type semiconductors is studied adequately [1, 2] and is attributed to the formation of a transistor quantum-dimensional structure similar to an Auger transistor at the semiconductor surface

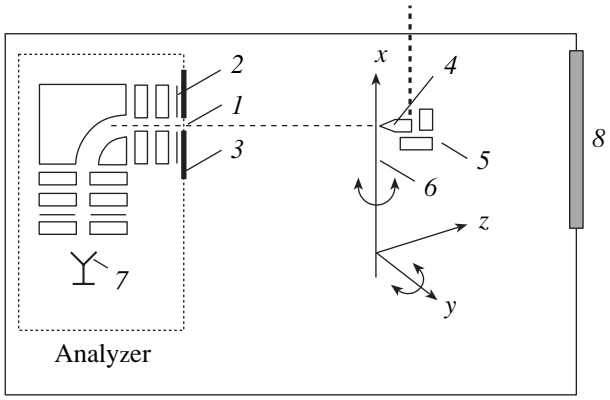

Fig. 1. Schematic representation of the energy analyzer for field-emitted electrons: (*1*) the probe orifice; (*2*) the anode; (*3*) the screen; (*4*) the emitter; (*5*) a cooling system; (*6*) a manipulator with five degrees of freedom; (*7*) a VÉU-6 secondary-electron multiplier; and (*8*) an ultrahigh-vacuum window.

in vacuum, whereas an increase in the quantum efficiency in the field-assisted photodetectors based on the n-type semiconductors required a special investigation.

Our studies of electron tunneling from n-type semiconductors in the high and ultrahigh electric fields have shown that the currents of emission from the n-type semiconductors both into vacuum (the n-GaAs tips) and into the metal (the tunneling MIS diodes based on n-Si) appreciably exceed the values expected in the case of electron emission from the conduction band.

It is typical that the studies of field emission from semiconductors are mostly restricted to the measurements and analysis of the current–voltage (I–V) characteristics. The data are interpreted in the context of the Stratton theory for semiconductors based on the classical Fowler–Nordheim theory of the tunneling field emission [10, 11]. Various deviations of the I–V characteristics from linearity (on the semilogarithmic scale) are accounted for by various electronic processes related to the penetration of an external electric field into the semiconductor. Additional and reliable data are needed for gaining insight into the phenomenon of electron emission from semiconductors and for practical use of this phenomenon.

In this paper, we report the results of studying the energy spectrum of electrons emitted from the atomically clean surface of n-GaAs single crystals. The energy distribution of electrons (EDE) in the course of the field emission yields direct information about the energy of electrons in an n-type semiconductor that are involved in the emission-current formation. A study of the EDE spectra would make it possible to test experimentally a model of tunneling emission suggested by us; in this model, the major contribution to the emission current is made by electrons from the valence band of the semiconductor.

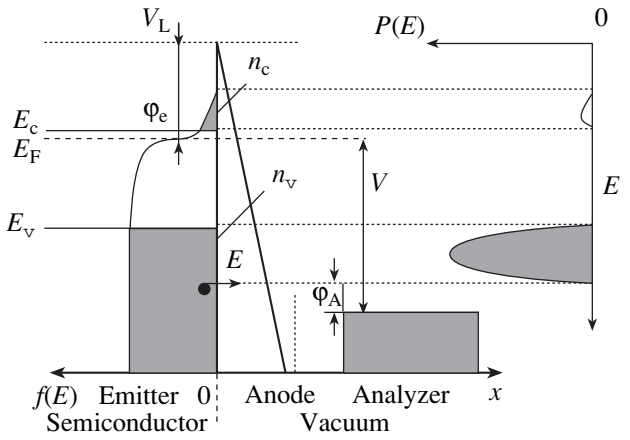

Fig. 2. The energy diagram of a field semiconductor emitter and the measured density spectrum of EDE $P(E)$ in the case of emission of electrons from the semiconductor into vacuum (the x axis). The following notation is used: φ_A is the work function for the analyzer; φ_e, work function for the emitter; E_F, Fermi level for the emitter; V_L, the vacuum level; V, the voltage between the emitter (semiconductor) and the analyzer (the electron collector); $f(E)$, the Fermi–Dirac distribution function at a temperature T; n_v and n_c, the electron concentrations in the valence and conduction bands, respectively; E_c, the conduction-band bottom; and E_v, the valence-band top.

2. EXPERIMENTAL

A study of the field emission from a semiconductor is typically restricted to measurements of the total emission current in relation to the voltage applied to the cold cathode with reference to the anode. In order to measure the current from different areas of the tip's emitting surface, we complemented measurements of the I–V characteristics with the method of probe scanning of the emission image, in which case emission from any surface area can be brought out to the entrance of a field electron spectrometer through the orifice 0.5 mm in diameter using a manipulator with five degrees of freedom.

The energy spectra of emitted electrons $P(E)$ were recorded using an electron field spectrometer with a spherical 135° analyzer.

The spectrometer's resolution was 0.02 eV (at the energy of emitted electrons $E = 3$ keV); it is noteworthy that the energy range of analyzed electrons was extended down to 4 eV below the Fermi level E_F. The retarding-potential method used in conjunction with the analyzer is illustrated in Fig. 2. A specific feature of this method consists in the fact that electrons leave the semiconductor as a result of tunneling penetration through the potential barrier at the semiconductor–vacuum interface, are accelerated by an external electric field on their way to the anode, pass through the probe orifice in the anode, are slowed down by the retarding field, and arrive at the analyzer's collector with an energy that exceeds the potential-barrier height at the analyzer–vacuum interface; this height is governed by the analyzer's work function φ_A in the case where the corresponding bias voltage V is applied to the semiconductor in reference to the analyzer (see Fig. 2). Therefore, the spectral curves for electrons that left the semiconductor with the energy corresponding to E_F have their origin at the bias potential $V = \varphi_A$, whereas the current detected by the analyzer sets in at the potential $V = \varphi_A + (E_v - E_F)$ for the electrons emitted, for example, from the valence-band top (E_v). Thus, the Fermi level of the semiconductor can be used as the relative level for the energy origin since its relative position in reference to the analyzer's Fermi level depends only on the applied voltage. It is worth noting that the analyzer's Fermi level and the value of φ_A were determined experimentally in the situation where the analyzer's cathode was, rather than the semiconductor, a reference tungsten cathode with a known work function.

The experiment was controlled and the data were processed using a specially developed detection system described in detail in [12] and a software package that took into account the specific features of semiconductor field cathodes [13].

The workpieces for cathodes had the dimensions $1 \times 1 \times 15$ mm and were cut from n-GaAs:Sn single crystals that had the resistivity of 0.001 Ω cm and were oriented along the ⟨100⟩ crystallographic direction. The workpieces were subjected to chemical etching in the 1 : 3 mixture of hydrofluoric and nitrous acids with the addition of doubly deionized distilled water; the temperature of the solution could be varied.

The energy spectra of electrons were measured with the samples placed in an ultrahigh-vacuum chamber at a residual pressure of $\leq 5 \times 10^{-10}$ Torr; the chamber was evacuated at temperatures that excluded any variations in electrical properties of the starting semiconductor single crystal. Stabilization of emission properties of the tip during collection of the emission current and cleaning of the surface was attained by field-assisted desorption so that an atomically clean emitting surface was obtained. The degree of cleanness of the surface was evaluated from reproducibility of the I–V characteristics and EDE and also from the symmetric emission image that is characteristic of crystals; this image can be observed on a luminescent display mounted in the high-vacuum chamber of the spectrometer. Using the tip's manipulator with five degrees of freedom (Fig. 1), we could measure the energy spectra of electrons emitted from any area of the active surface with visual inspection of the surface's state in a field electron microscope. Measurements were carried out only if the I–V characteristics and EDE were reproducible in the chosen range of operating voltages. The spectra of electrons were recorded under conditions of repeated scanning with the energy step of 37 meV in the energy range from 0 to 4 eV below the Fermi level E_F in order to cover the entire energy range of electrons involved in the formation of the field-emission current.

It is worth noting that a study of the EDE in the case of emission from a semiconductor is a much more complicated experimental challenge than the corresponding studies of EDE for the field cathodes made of metal. One of the main difficulties consists in the necessity to correct the potential applied to electrostatic lenses of the spectrometer by the voltage drop across the semiconductor in the course of the current collection during measurements. Therefore, in order to control automatically the voltage and analyze the EDE, we developed in this study a special software package named FEESA (field electron energy spectrum analyzer) and a precision system of detection. The FEESA software makes it possible to analyze a practically unlimited volume of collected data and choose the operating-mode characteristics such as the energy resolution, the voltage step in the case of the EDE scanning, and the time interval of collection in relation to the signal level (to the mode of counting separate electrons up to 10^6 electrons per second). The merits of this software are described in detail in [13].

Tunneling currents in the MIS transistor structures were studied for the Al–SiO_2–*n*-Si structures based on *n*-Si with the resistivity of 0.3 Ω cm. The tunneling-transparent oxide layer was grown in a flow of dry oxygen at comparatively low temperatures (600–700°C). According to the data of ellipsometric measurements, the geometric thickness of the SiO_2 layer was ~2 nm. The *I–V* characteristics were measured in the common-emitter configuration. The experimental conditions were described in detail in [5]. The conclusion concerning the efficiency of the MOS emitter (the injection factor $\gamma > 0.5$) was arrived at after a comparative analysis of recombination-radiation intensity for the silicon MIS diode structures (with various metals deposited on the tunneling-thin layer of silicon oxide) and silicon diodes with the diffusion p^+–*n* junctions in relation to the current density [3].

3. RESULTS

3.1. Energy Distribution of Electrons in the Case of Tunneling in an n-GaAs–Vacuum System

The energy spectra of the electrons emitted to vacuum were measured at successive stages of cleaning the GaAs surface using the field-desorption method. The EDE spectra have a characteristic shape with a single peak (Fig. 3); as the cleaning of the surface progresses, the positions of the peak and the low-energy edge of the spectrum shift towards the Fermi level energy E_F ($E = 0$) (curves *1–3*). The spectra shown in Fig. 3 are normalized to the peak and are represented in arbitrary units. In the case of emission of electrons from the atomically clean GaAs surface, the low-energy edge of the EDE spectrum corresponds to the energy level E = 1.4 eV below the Fermi level E_F (see Fig. 2). The initial position of the EDE spectra for a semiconductor coated with a thin oxide layer depends on the voltage drop across the oxide layer.

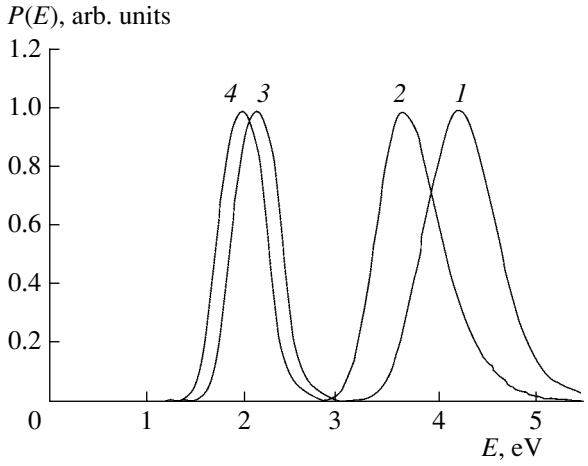

Fig. 3. Experimental EDE spectra for *n*-GaAs: (*1*) the emitter coated with a layer of natural oxide, (*2*) an intermediate stage of cleaning of the GaAs surface, (*3*) the emitter with atomically clean surface (U_a = 2 kV), and (*4*) the same at U_a = 1.4 kV. The energy is measured with respect to E_F.

As the anode voltage U_a decreases, the spectra are shifted along the energy scale (see Fig. 3); however, the edge of the spectra is always limited by the energy level E = 1.4 eV (curve *4*), which corresponds to the valence-band top E_v for GaAs. This statement is based on the value of the band gap for GaAs (E_g = 1.4 eV) and on the principle of measurements by the method of retarding potential. As mentioned above, energies in the EDE spectra are measured from the Fermi level of the emitter in this case; the Fermi level closely coincides with the conduction-band bottom (E_c) for the heavily doped crystal under study.

In the case of tunneling emission in the crystallographic direction ⟨100⟩, the electron spectra feature a single peak, are well reproduced in repeated measurements, and remain invariable after several hours after cleaning of the surface by the field-assisted desorption and at a high anode voltage, in which situation the GaAs single crystals are evaporated. Moreover, the shape of the spectra is changed only slightly in the case where the emitter is rotated by an angle as large as 60° with respect to the direction of the single-crystal axis. An analysis of the spectra of electrons emitted from other areas of the surface shows that the low-energy edge of the EDE spectra is always located at the energy E = 1.4 eV. Thus, the analysis of the results suggests that the major contribution to the tunneling current from the *n*-GaAs single crystals is made by electrons emitted from the valence band within the range of kT (k is the Boltzmann constant and T is absolute temperature) below the valence-band top; insignificant discrepancies between the spectra corresponding to different crystallographic planes are related to specific features of tunneling from deeper energy levels. The

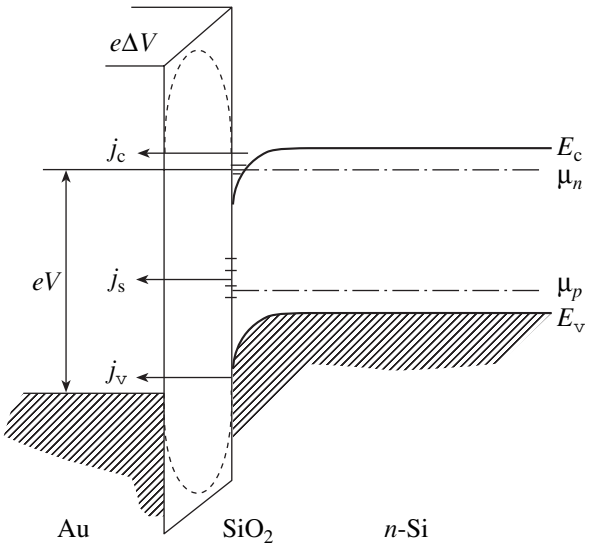

Fig. 4. The energy-band diagram for a silicon MIS diode with a tunneling-transparent oxide layer in the case of a forward bias. A voltage V is applied to the structure; the voltage drop across the oxide $\Delta V \geq 1$ V; j_c, j_s, and j_v are the tunneling electron currents into metal from the semiconductor's conduction band, from the surface states in the band gap, and from the valence band, respectively; and μ_n and μ_p are the quasi-Fermi levels.

experimentally obtained width of the EDE curves at the half-maximum (FWHM) (0.6–0.8 eV) coincides also with the value predicted by the Stratton theory for emission from the valence band.

The results obtained are consistent with the physical model developed previously by us for tunneling currents in the semiconductor–vacuum and MIS structures; the characteristic feature of these structures consists in the predominant contribution of the valence-band electrons to tunneling emission from a semiconductor in the case where the semiconductor acts as the cathode. Our results confirm the validity of this model.

3.2. Tunneling Emission Currents in the MIS Diodes

Our previous studies of the electron emission in silicon MIS diodes with a tunneling-transparent oxide layer showed that predominant injection of electrons from the silicon valence band into metal occurs in the case of forward bias voltage applied to the structure (positive potential at the metal) if the voltage drop across the oxide ΔV is such that $e\Delta V > E_g - E_F$, where E_g is the silicon band gap and E_F is the Fermi level in silicon (Fig. 4) [3].

For such a bias voltage and for a relatively thick insulator layer (2 nm), the electron-emission current from the valence band of the semiconductor to the metal can be generally represented (according to [14]) in the form of the hole current from the metal to the semiconductor's valence band

$$j_p = (4\pi m_{th} q/h^3) \times \int_{-\infty}^{+\infty} [f_m(E) - f_s(E)] \int_0^E T(E_x) dE_x dE, \quad (1)$$

where f_m and f_s are the Fermi functions for the metal and semiconductor, respectively; $T(E_x)$ is the probability of tunneling of valence electrons from the semiconductor to the metal; E_x is the energy component in the direction of the x axis (i.e., perpendicularly to the barrier); E is the total energy; and m_{th} is the effective mass of holes that penetrate through the barrier. With the proviso that $e\Delta V > E_g - E_F$, the hole injection current is in fact the current of electrons from the semiconductor's valence band that tunnel into the metal; the energy of these electrons E is in the range $E_{Fm} < E < E_v$ (E_{Fm} and E_v are the Fermi level in the metal and the valence-band top in the semiconductor, respectively). In this case, the simplified form of expression (1) can be written as

$$j_p \approx (4\pi m_{th} q/h^3) \exp(-\chi_h^{1/2} d) \int_{E_{Fm}}^{E_v} E dE, \quad (2)$$

where χ_h is the barrier height for "metal" holes and d is the effective thickness of the oxide.

It is worth bearing in mind that the effective mass of holes in the valence band of silicon oxide exceeds more than fivefold the effective mass of electrons. As a result, we should consider the tunneling of charge carriers from the semiconductor's valence band into metal only as transitions of electrons from the valence band through the oxide's conduction band rather than the valence band. Therefore, the value of E_g in the semiconductor should be added to the insulator–semiconductor barrier height.

4. DISCUSSION AND CONCLUSIONS

It is worth noting that the issue of whether the field-emission current is formed by electrons from the valence band or from the conduction band has not been settled unambiguously until now. Prior to the results obtained in this study, it was widely believed [15] that the main contribution to the tunneling emission current is made by electrons from the conduction band for low-resistivity n-type semiconductors (even more so for almost degenerate semiconductors, as in the case of GaAs under consideration). Our results do not support this belief. Moreover, we assume that it is the electron emission from the valence band that represents a characteristic feature of the field emission from semiconductors where the current depends on illumination of the emitter (a photofield cathode). We now substantiate this statement.

One of the causes of absence of electrons from the conduction band in the EDE spectra can be a lower electron concentration in the conduction band compared to that in the valence band ($n_c = 5 \times 10^{18}$ cm^{-3} and $n_v = 10^{22}$ cm^{-3}, respectively), which yields the relation between the currents from the valence and conduction bands $j_v \gg j_c$, in which case it can be difficult to measure the value of j_c experimentally. However, the high accuracy of the performed measurements (an unlimited signal integration on the level of counting of separate electrons, for example, for measuring the value of j_c) makes it possible not only to measure even lower currents but also to measure the EDE for the signals that differ by six–eight orders of magnitude from each other. In other words, the absence of electrons from the conduction band in the EDE spectra is not related to disadvantages of the measuring system.

It is worth noting that the absence of electrons from the conduction band in the EDE spectra for another semiconductor, germanium, with the (100) face orientation is accounted for by specific features of the conduction-band structure [15]. In germanium, the equienergy surfaces near the conduction-band bottom are represented by ellipsoids whose centers are distanced from the coordinate origin in the $\langle 111 \rangle$ direction. The components of the vector $\mathbf{k}$ are parallel to the (100) plane, so that the corresponding states are not located in the central region of the surface Brillouin zone for the unreconstructed surface [15]. As a consequence of a large tangential-energy component related to these states, the normal energy component for an electron at the conduction-band bottom is appreciably smaller than the energy of an electron with $\mathbf{k}_{\|} \approx 0$ at the top of the valence band. The probability of tunneling in the x direction $D(E - E_\perp)$ for an electron that has the energy E and is incident on the barrier, where $E_\perp = (p_y^2 + p_z^2)/2m$ and p_y and p_z are the tangential components of the electron's quasi-momentum, is governed only by the energy $E_\perp$ related to the normal component of velocity. Therefore, if $E_\perp$ is fairly large, the probability of emission from the conduction band is low, as occurs for the (100) plane of germanium; consequently, $j_v \gg j_c$ even in the case of a degenerate electron gas in the conduction band of germanium.

However, if it is assumed that, in the case under consideration as well, the absence of electrons from the GaAs conduction band in the EDE spectra is also related to a specific feature of the energy-band structure, we should expect there to be significant differences between the experimental EDE spectra in different crystallographic directions, which was not observed experimentally. Moreover, it should be emphasized that electrons from the conduction band were not detected in the EDE spectra measured in different directions in the studies of Si [16, 17] and Ge [18–20]. In the study reported in [19], the accuracy of measurements was so high that the EDE fine structure was observed for germanium and was related to the band of surface states; however, emission from the conduction band was not observed for either of the studied crystallographic directions.

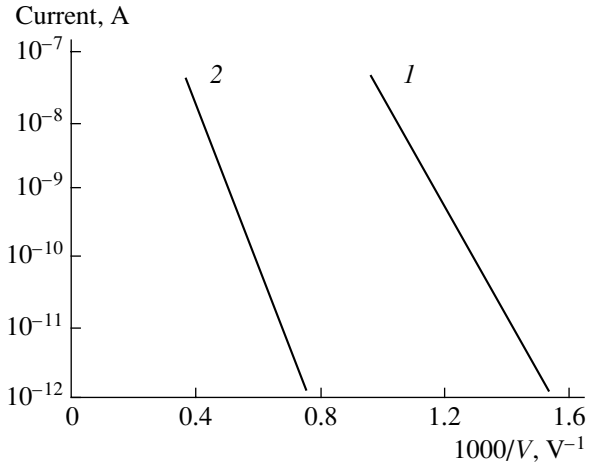

Fig. 5. The current–voltage characteristics for the emission current in (*1*) GaAs with a layer of natural oxide and (*2*) GaAs with atomically clean surface.

The levels of the valence and conduction bands in the semiconductor's bulk are found to be located at the same energy in ultrahigh electric fields (up to 5×10^7 V/cm and higher) required for field emission from semiconductors. As a result, the tunneling current within the semiconductor near its surface can be considered as the Zener breakdown. However, the linear shape of the I–V characteristic plotted on the logarithmic scale (Fig. 5) for the studied low-resistivity GaAs crystal indicates that the role of the effects related to penetration of the field into the semiconductor's bulk is insignificant, at least for the total emission current. It is worth noting that a possible mechanism of the tunneling emission current in n-GaAs may also involve the electron–hole recombination at the surface via surface states in the band gap or the direct interband recombination at the surface, which can undoubtedly reduce the electron emission current from the conduction band. However, this issue requires an additional investigation. Experimental studies show that electrons forming the tunneling current leave for vacuum with the energies that correspond to the top of the valence band, whereas the electron emission from the conduction band of heavily doped n-GaAs is not observed. This conclusion is confirmed both by the presence of unidirectional tunneling injection in silicon diodes with the tunneling-transparent intermediate oxide layer at a positive voltage applied to the metal (for an n-type semiconductor), irrespective of what type of the metal was deposited, and by the development of an Auger transistor whose unique properties are based on the efficient Al–SiO_2–n-Si emitter with the tunneling-transparent oxide layer.

In conclusion, we should note that the results of the studies reported in this paper make it possible to

address directly the solution of the theoretical and experimental problem related to the emission of electrons in high electric fields; this problem is common for both Auger transistors and the field needle-shaped semiconductor emitters.

ACKNOWLEDGMENTS

This work was supported in part by the Federal Agency for Science and Innovations of the Russian Federation (state contract no. 02.434.11.2027) and by a grant of the President of the Russian Federation (grant no. NSh 2223.2003.2).

REFERENCES

1. A. A. Rogachev, V. D. Kalganov, N. V. Mileshkina, and E. V. Ostroumova, Microelectron. J. **31**, 905 (2000).
2. V. D. Kalganov, N. V. Mileshkina, and E. V. Ostroumova, Fiz. Tekh. Poluprovodn. (St. Petersburg) **37**, 372 (2003) [Semiconductors **37**, 354 (2003)].
3. I. V. Grekhov and E. V. Ostroumova, Pis'ma Zh. Tekh. Fiz. **12**, 1209 (1986) [Sov. Tech. Phys. Lett. **12**, 501 (1986)].
4. I. V. Grekhov, E. V. Ostroumova, A. A. Rogachev, and A. F. Shulekin, Pis'ma Zh. Tekh. Fiz. **17** (13), 44 (1991) [Sov. Tech. Phys. Lett. **17**, 476 (1991)].
5. E. V. Ostroumova and A. A. Rogachev, Fiz. Tekh. Poluprovodn. (St. Petersburg) **28**, 1411 (1994) [Semiconductors **28**, 793 (1994)].
6. E. V. Ostroumova and A. A. Rogachev, Microelectron. J. **29**, 701 (1998).
7. T. Ando, A. B. Fowler, and F. Stern, Rev. Mod. Phys. **54**, 437 (1982).
8. V. D. Kalganov, N. V. Mileshkina, and P. G. Shlyahtenko, J. Phys.: Condens. Matter **15**, 5171 (2003).
9. V. D. Kalganov and T. V. Mileshkina, RU Patent No. 2248066 (2005).
10. K. L. Jensen, Vac. Sci. Technol. B **13**, 516 (1995).
11. R. Stratton, Phys. Rev. [Sect. A] **135**, 794 (1964).
12. V. D. Kalganov and N. V. Mileshkina, Radiotekh. Élektron. (Moscow) **45**, 1487 (2000) [J. Commun. Technol. Electron. **45**, 1347 (2000)].
13. V. D. Kalganov, N. V. Mileshkina, E. V. Ostroumova, and E. A. Rogacheva, in *Proceedings of MRS-2002 Full Meeting* (Boston, USA, 2002), Paper M5.25; V. D. Kalganov, N. V. Mileshkina, S. A. Sapronov, et al., in *Proceedings of 24th International Conference on Microelectronics (MIEL 2004)* (Nis, Serbia and Montenegro, 2004), Vol. 2, p. 195.
14. H. C. Card and E. H. Rhoderick, Solid-State Electron. **16**, 365 (1973).
15. A. Modinos, *Field, Thermionic and Secondary Electron Emission Spectroscopy* (Plenum, New York, 1984; Nauka, Moscow, 1990).
16. B. F. Lewis and T. E. Fisher, Surf. Sci. **41**, 371 (1974).
17. A. Modinos, Prog. Surf. Sci. **42**, 45 (1993).
18. V. D. Kalganov, N. V. Mileshkina, and S. A. Sapranov, Phys. Low-Dimens. Semicond. Struct., No. 11/12, 89 (1996).
19. T. Deck, V. D. Kalganov, N. V. Mileshkina, and A. Moscardini, Phys. Low-Dimens. Semicond. Struct., No. 5/6, 187 (1998).
20. V. D. Kalganov, N. V. Mileshkina, and S. A. Sapronov, Vacuum **46**, 559 (1995).

Translated by A. Spitsyn